HIGH PRESSURE EFFECT ON 3D TOPOLOGICALLY NONTRIVIAL SYSTEMS WITH MAGNETIC IMPURITIES

I.K. KAMILOV[1], L.A. SAYPULAEVA[1], N.V. MELNIKOVA[2], A.I. RIL[3], S.F. MARENKIN[3,4], Sh.M. ALIEV[1]

[1]Institute of Physics, DFRC RAS, 367015, Russia, Republic of Dagestan M. Yaragskogo str. 94, Makhachkala, Russia.

[2]Ural Federal University, Institute of Natural Sciences and Mathematics Yekaterinburg, Russia 620002

[3]Kurnakov Institute of General and Inorganic Chemistry, Russian Academy of Sciences Moscow 119991

[4]National University of Sciences and Technology "MISIS", Moscow 119991

e-mail:l.saypulaeva@gmail.com

The main results of investigations on the electrical and magnetoresistance (MS) of a composite material consisting of 70 mol. % Dirac half-metal Cd_3As_2 and of 30 mol. % ferromagnetic MnAs are presented at pressures up to 50 GPa in a high-pressure chamber with diamond anvils of the "rounded cone-plane" type, as well as magnetization at hydrostatic pressures up to 6 GPa in a "Toroid" high-pressure chamber, both in the room temperature mode and in the temperature range from 180 to 350 K at atmospheric pressure. A 4:1 methanol-ethanol liquid is used as the pressure transmitting agent. The elemental analysis of Cd_3As_2 composite + *30* mol% MnAs, reveals that most of the volume is Cd_3As_2 phase. The share of MnAs phase inclusions is less than 5%. The presence of a significant non-mixing region of the Cd_3As_2 and MnAs melt phases is the peculiarity of Cd_3As_2+MnAs.

With increasing the pressure, a negative magnetic resistance (MR) is observed in the whole considered baric region. The maximum of the negative MR is manifested in the pressure region of 22-26 GPa. Further increase in pressure up to a maximum pressure produces several extrema on the $\Delta R/R_0(P)$ curve, and the negative MR does not exceed 4%. In the pressure drop mode from 50 GPa, the baric dependence $\Delta R/R_0(P)$ is characterized by inversion of the MR sign: the negative MR is replaced by a positive one at about 40 GPa, and the maximum value of the positive MR ~5.3 % is observed near 20 GPa. Signs of instability of the Cd_3As_2 monoclinic structure due to its partial decomposition during decompression are determined. The prevailing negative MR over a wide pressure range of 16-50 GPa is discussed to be irrespective of the MnAs clusters effect, since the magnetic transformation observed in MnAs occurs at pressures lower than 1 GPa, and the magnetization decreases with further pressure increase up to 5 GPa.

Keywords: electric resistance, clusters, high pressures, magnetoresistance

INTRODUCTION

In recent years, the 3D topologically nontrivial systems with magnetic impurities, Dirac and Weyl semimetals, have become a new focus of condensed state physics. This is not surprising in view of that the elements of the II and V groups of the periodic system form chemical compounds exhibiting very interesting semiconductor properties [1]. A special group is formed by ternary and quaternary alloys, whose properties depend on the properties of the binary compounds presented in their composition. The II_3-V_2 group is the best known among II-V alloys: doping Cd_3As_2, Zn_3As_2 by Mn generates magnetic semiconductors $(Cd_{1-x}Mn_x)_3As_2$, $(Zn_{1-x}Mn_x)_3As_2$, $(Cd_{1-x-y}Zn_yMn_x)_3As_2$ [2, 3].

Today the physical properties of these materials are not fully understood. The goal of the present work is to research the high-pressure effect on a 3D topologically non-trivial system with magnetic impurities on the case of $(Cd_{1-x}Mn_x)_3As_2$ solid solution.

The electrical and magnetic properties of $(Cd_{1-x}Mn_x)_3As_2$ composites are largely determined by MnAs nanoclusters. These composites are characterized by the metallic type of conductivity. It can be noted that the electrical resistivity of a number of composites decreases with growth in the magnetic field. This behavior is observed both at low temperatures and at room temperature, which indicates spin-dependent scattering mechanisms and exchange interaction of unknown nature between magnetic nanoclusters of the composite.

The investigations of Cd_3As_2 show the topological aspect of electrical properties [4 -6]. The valence and conduction bands of Cd_3As_2 are the conical structures intersecting near the Γ point at the Fermi level. The regions where the cone-shaped structures indicate the formation of 3D Dirac points are identified by the angular resolution photoelectron spectroscopy (Fig. 1).

Figure 2 presents the zone structure of α-Cd_3As_2 tetragonal phase which is typical to a Dirac semimetal. The figure shows that the Λ6 and Λ7 zones intersect to the left of the Γ point at the Fermi level, which results in the formation of a 3D Dirac cone.

Previously [9], Cd_3As_2 was considered as a narrow-gap semiconductor with electronic conductivity and high charge carrier mobility μ =15000 $cm^2/(V\ s)$.

131, H.Javid ave, AZ-1073, Baku
Institute of Physics
E-mail: jophphysics@gmail.com

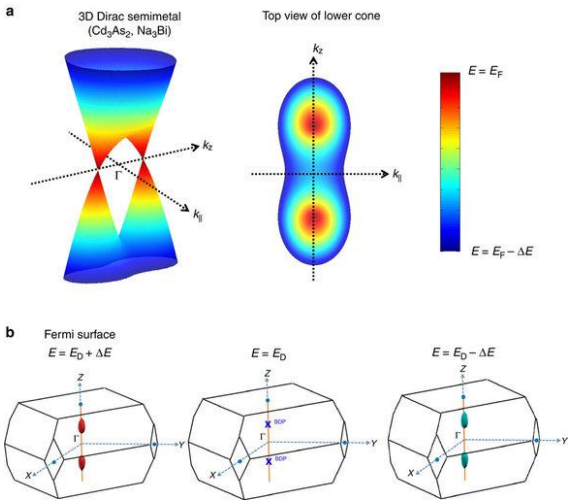

Fig. 1 - (a) Illustration of three-dimensional sputtering of a Dirac half-metal. (b) Scheme of the Fermi surface above the Dirac point, at the Dirac point and below the Dirac point [7]

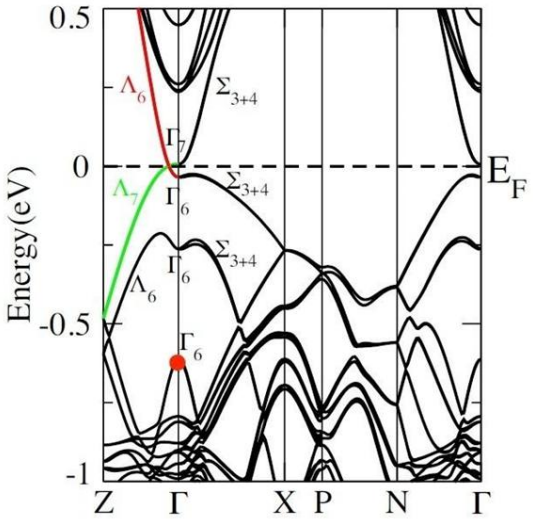

Fig. 2. The zone structure of α-Cd_3As_2 (*$I4_1/cd$*) [8]

The electron transport properties of Cd_3As_2 reveal unexpected properties [10-12]: despite the high mobility of current carriers, the thermal conductivity of Cd_3As_2 appeared to be lower than the value of 4.17 W/m·K. The reason for this discrepancy is believed to be a large electron-phonon scattering. The thermal conductivity is usually by an order of magnitude higher for common metals or semi-metals with similar electrical conductivity.

Hall effect measurements [5] reveal the high mobility of electrons up to 180 cm^2 /V·s at room temperatures and to 134 cm^2 /V·s at 3 K. The carrier density is within the order of 10^{19} cm-3. The Seebeck coefficient (S) shows a negative sign indicating the n-type conductivity: S reaches 74.1 μV/K at room temperature, and the temperature dependence of S(T) is linear over a wide temperature range (2-380 K).

Measurements of electrical resistivity in Cd_3As_2 monocrystals under pressures up to 50.9 GPa proves that after an initial increase in pressure, the low-temperature resistivity begins to decrease at pressures above 6.4 GPa and the superconductivity appears at 8.5 GPa with Tc ≈2.0 K, which increases with pressure and reaches a maximum value of 4.0 K at 21.3 GPa [6].

Manganese dissolves in Cd_3As_2 forming a wide range of ternary solid solutions $(Cd_{1-x}Mnx)_3As_2$ in a certain concentration range [13]. Exceeding the limiting concentration leads to the formation of a eutectic alloy containing, along with the solid solution $(Cd_{1-x}Mnx)_3As_2$, the nanoscale ferromagnetic inclusions of MnAs with a unit cell of symmetry *P63/mmc* and parameters a = 3.72 Å and c = 5.71 Å. At room temperature, MnAs undergoes a transition from hexagonal NiAs-type structure with *P63/mmc* symmetry to orthorhombic MnP-type structure with *Pnma* symmetry when the pressure reaches 0.45 GPa [14]. The high value of the Curie point in MnAs (318 K) makes it a promising material for application in various spin electronics elements functioning in the terahertz range [15-17].

SAMPLES AND EXPERIMENTAL METHOD

The synthesis of $(Cd_{1-x}Mnx)_3As_2$ crystals was performed by the vacuum-ampoule method from

Cd_3As_2 and MnAs compounds at the manganese arsenide melting temperature [18]. The samples were a composite consisting of nanoscale ferromagnetic MnAs pellets chaotically arranged in the volume of the Cd_3As_2 semiconductor matrix. The obtained samples were analyzed by X-ray diffraction and scanning electron microscopy (SEM). Elemental analysis of the investigated composites showed that the Cd_3As_2 phase constitutes the major part of the volume. The fraction of MnAs phase inclusions occupies less than 5%. When interpreting the peaks, it was found that the X-ray diffraction pattern contained two main phases: α-Cd_3As_2 - tetragonal and MnAs - magnetic hexagonal (Fig. 3).

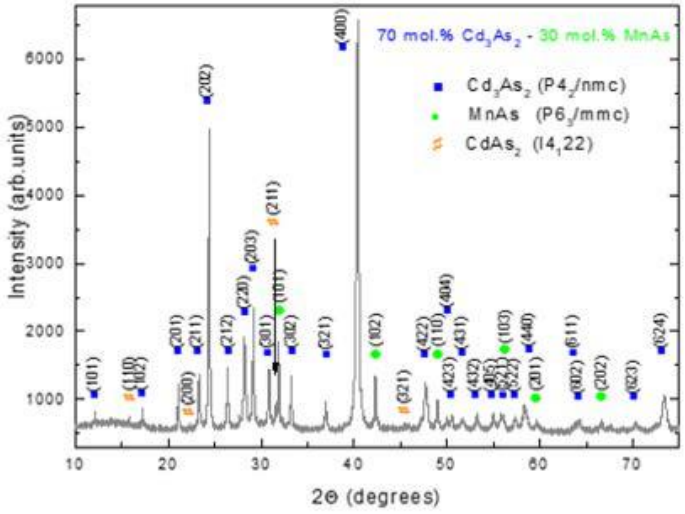

Fig. 3. X-ray diagram of the Cd_3As_2 + 30mol% MnAs sample.

There was also an insignificant amount of $CdAs_2$ phase present. Cd_3As_2 phase and Cd_3As_2+MnAs eutectic were observed on microstructures. The peculiarity of Cd_3As_2+MnAs was the existence of a significant non-mixing region of the Cd_3As_2 and MnAs melt phases.

The effect of high pressure on the electrophysical properties of composites was investigated in a high-pressure chamber (HPC) with diamond anvils of the "rounded cone-plane" type and in a high-pressure apparatus of the "Toroid" type. The measurement technique was described in detail in [19-13].

EXPERIMENTAL RESULTS AND DISCUSSION

Figure 4 depicts the pressure *P* dependence of $(Cd_{1-x}Mnx)_3As_2$ resistance *R* at two consecutive cycles of measurements (pressure rise and drope) in the room temperature region. The baric interval of 15-25 GPa of the first cycle is dominated by a significant decrease of *R* with increasing *P*. The resistivity in this pressure range varies almost linearly with the average rate *dR/dP*=-24.9 Ohm/GPa (Inset to Fig. 4).

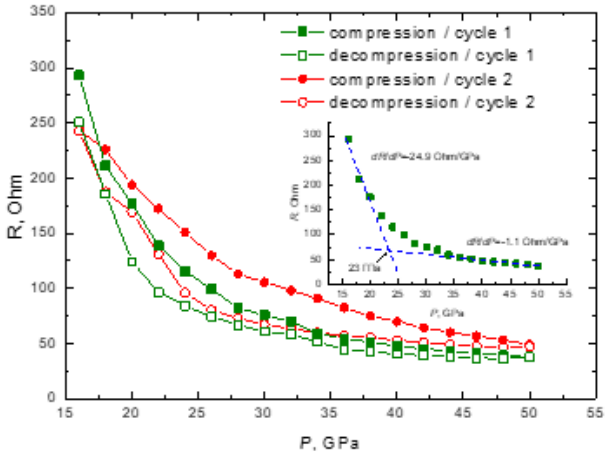

Fig. 4. Dependences of electrical resistivity of Cd_3As_2 + 30 mol% MnAs on pressure at two consecutive cycles of measurements. The inset shows the *R(P)* dependence of the first cycle at pressure rise. The dashed lines stand for the determination of the *dR/dP* slopes.

The predominance of *R* hysteresis in $(Cd_{1-x}Mnx)_3As_2$ in the pressure range of 15-50 GPa seems to be rather interesting, as it may testify to the structural transition occurring in Cd_3As_2, whose structure above 4.67 GPa is already monoclinic (*P21/c*) [6]. However, based on the X-ray diffraction data given in [6], the monoclinic phase is registered up to 17.8 GPa, while its predominance up to 50 GPa is only hypothetical.

Figures 5 show the field dependences of MR measured at different pressures up to 50 GPa and in magnetic fields up to 1 T at room temperature. The measurements are carried out in the pressure rise and drope modes, which allow us to qualitatively determine the relationship between the observed hysteresis in the *R(P)* dependence and the MR behavior. The magnitude of the transverse MR is estimated by the formula

$$MR = 100 \cdot \frac{R(B)-R(0)}{R(0)},$$

where *R*(*B*) is the electric resistivity in the transverse magnetic field with induction *B*, R(0) is the electrical resistance in the absence of the magnetic field.

As follows from Fig. 5, a positive MR is observed in the composite at *P*=16 GPa. A similar positive MS in Cd_3As_2 + *30* mol% MnAs was previously observed under a relatively low pressure of 7.7 GPa, which was attributed to the competition between the influence of the Lorentz force and the spin-dependent scattering of charge carriers on MnAs clusters [24]. This positive MR appears to extend up to16 GPa, however, its magnitude gradually decreases. Further growth of *P* changes the sign of MR and the maximum value of negative MR ~20% is registered at 22 GPa in the 1 T field. It should be noted that in this pressure region there is a sharp change of the *dR/dP* rate on the *R(P)* dependence and the cutoff intersection crossing of the approximation lines of low and high pressure regions correspond to the value of ~23 GPa (Inset to Fig. 4).

The maximum of the pressure-induced negative MR is realized in the relatively narrow pressure region of 22-26 GPa, and further at *P*>26 GPa the negative MR does not exceed 4% at 38 GPa. The dynamics of this negative MR change at pressure rise appears ambiguous, since there are several local minima on the $\Delta R/R_0(P)$. dependence. At pressure relief, the field dependence of MR exhibits an inversion of a sign at *P*>40 GPa (Fig. 5) and a maximum positive MR of ~5.3 % is observed around 20 GPa. So, the change of the MR sign at pressure rise and release may indicate that in Cd_3As_2 + 30 mol% MnAs there is an irreversibility of structural properties due to partial decomposition of the composite after decompression. At the same time, the presence of negative and positive MR maxima is presumably related to the nature of phase transformations in the electronic subsystem of the composite [25].

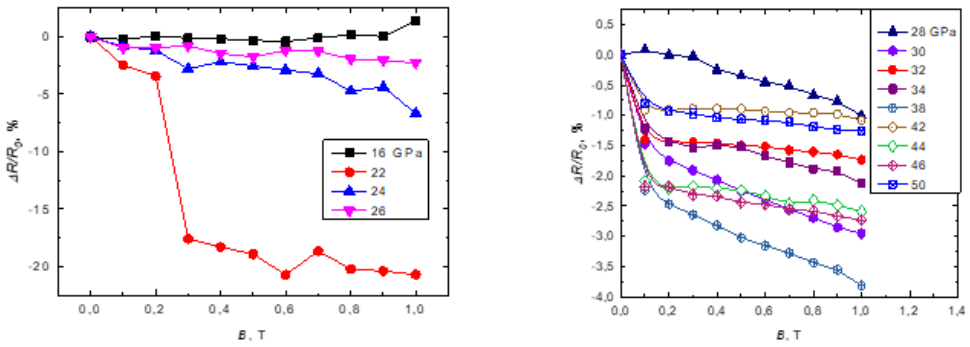

Fig. 5. Dependences of the magnetoresistance of Cd_3As_2+*30* mol% MnAs on the magnetic field induction in the pressure range of 16-26 GPa (upper panel) and 28-50 GPa (lower panel) measured in the pressure rise mode.

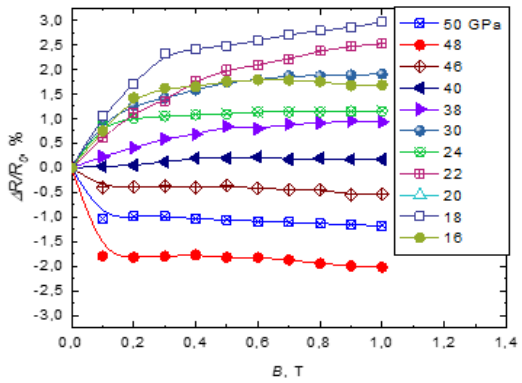

Fig. 6. The dependences of the Cd_3As_2+30 mol% MnAs magnetoresistance on the magnetic field induction at some fixed pressure values measured in the pressure relief mode.

We further note that the existence of MnAs clusters in the composite structure can somehow have a bearing on the nature of addressed MR. However, their magnetic behavior remains unclear in the considered pressure ranges from 15 to 50 GPa.

This is explained by that the magnetic phase diagram for the MnAs bulk compound is well studied only up to 1.1 GPa at present [26]. According to neutron studies, it is reported that the orthorhombic phase of the MnP type remains stable up to 1.26 GPa, where a spiral structure with the propagation vector $\tau_a = 0.125 \times 2\pi \times a^*$ is further formed [27]. As the study of the MnAs cluster magnetic properties at pressures comparable to the MR measurements (Fig. 5) is extremely difficult, our measurements of the isothermal magnetization are limited to the region up to 5 GPa.

An analogy between bulk MnAs compounds and MnAs clusters is found by investigating the temperature dependence of the magnetization $M(T)$. Fig. 6 shows the dependence of $M(T)$. measured in magnetic fields H up to 3.6 kE at atmospheric pressure. The qualitative course of the curve is identical: there is a sharp increase in M near $T_C \approx 318$ K upon cooling, which is associated with the magnetic transformation from a nonmagnetic to a ferromagnetic state [26]. Increase in the field up to 3.6 kE initiate a slight shift of the Curie temperature toward high temperatures up to T_C =321 K (defined as dM/dT for M curves in heating mode). This behavior confirms that MnAs nano-inclusions in the Cd_3As_2 matrix exhibit similar magnetic properties as in their bulk counterpart. At the same time, a remarkable feature of the ferromagnetic transition is the absence of the characteristic hysteresis M, which is an evidence of the first order phase transition in bulk MnAs. This magnetic transition occurs with the change of β (orthorhombic) nonmagnetic phase into α (hexagonal) ferromagnetic phase, accompanied with a hysteresis width of about 8-12 K. But, the absence of hysteresis M may be equivalent to the situation occurring in epitaxial layers of MnAs(001)/GaAs(111), in which the coexistence region of $\alpha+\beta$ phases prevails [28].

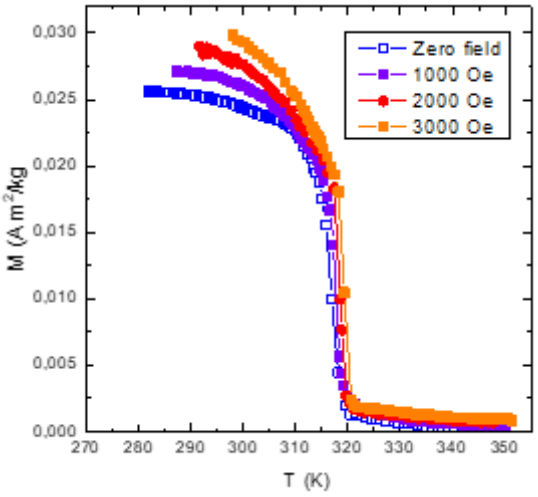

Fig. 7. The dependences of the Cd_3As_2+*30* mol% MnAs magnetoresistance on pressure at different values of the transverse magnetic field induction up to B=1 T.

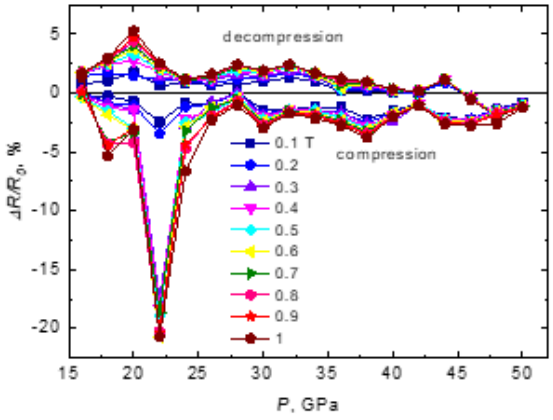

Fig. 8. The temperature dependence of the Cd_3As_2+*30* mol% MnAs magnetization in the region of the paramagnetic to ferromagnetic transition measured in magnetic fields up to H=0 - 3.6 kE. The curves of successive heating and cooling cycles are shifted relative to each other.

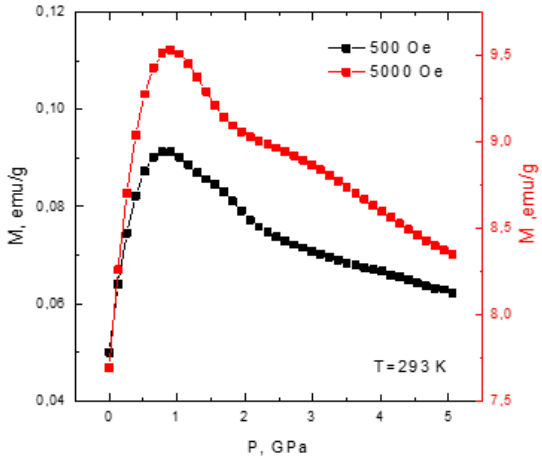

Fig. 9. The baric dependence of the magnetization at T=293 K measured under magnetic fields 500 E and 5 kE.

The dependence of isothermal M on P at T=293 K is illustrated in Figure 7. At atmospheric pressure (P=0 GPa), the values M=0.05 Am^2/kg and M=7.69 Am^2/kg are maintained in magnetic fields of 500 E and 5 kE, respectively. The M maxima are observed on the $M(P)$ dependence, which indicate the realization of magnetic transformation occurring in MnAs clusters. The increase of M reaches 80% in the region of maxima at H=500 E and 23% at H=5 kE from the initial values of M. In addition, the phase transition region shifts toward high pressure from P=0.77 GPa to P=0.9 GPa with increasing H. Such a prevailing trend indicates the change of the ferromagnetic state of MnAs clusters to the antiferromagnetic ordering.

The antiferromagnetic phase is a consequence of the metamagnetic transition, which can be induced by a simultaneous effect of H and P below T_C in the volume MnAs compound.

Based on observation that the further behavior of $M(P)$ demonstrates a gradual decrease up to 5 GPa (Fig. 7), one can conclude that MnAs clusters under higher pressure conditions are likely to be in a non-magnetic state. For this reason, it can be argued that the appearance of negative MR in the pressure range of 16-50 GPa (Fig. 5) should not be associated with the influence of MnAs clusters. On the other hand, it is worth noting that the Mn impurity has the ability to dissolve in the Cd_3As_2 matrix in an extremely minimal amount. In such a case, the negative MR arises due to the topological phase transition caused by the magnetic impurity and the formation of magnetic polarons, which support spin-dependent scattering in doped Cd_3As_2. For a more detailed analysis of the MR nature in Cd_3As_2 + *30* mol% MnAs, including the change of sign and predominance of pronounced maxima on the $\Delta R/R_0(P)$ dependence, it is required a clearer understanding of the influence of the Mn impurity on the zone structure and density of states in the Cd_3As_2 monoclinic phase.

CONCLUSION

The resistance and MR feature at high pressure up to 50 GPa, as well as the magnetic properties of MnAs clusters up to 5 GPa are investigated in Cd_3As_2 + *30* mol% MnAs composite. The measurement of R at cyclic P revealed a hysteresis in a wide range of pressures, which is associated with the instability of the monoclinic structure of Cd_3As_2 at P>16 GPa with its partial decomposition after pressure relief. This behavior is confirmed by the results of MR measurements at pressure rise and pressure drop, which show a change of the MR sign from negative to positive. The $\Delta R/R_0(P)$ dependence also shows pronounced MR maxima, in particular, at pressure increase the negative MR maximum is ~20% and at pressure relief the positive MR maximum is ~5.3%, the origin of which is most likely caused by the influence of magnetic Mn impurity as a result of topological phase transformation. The influence of magnetic MnAs clusters on the MR features in the range of 16-50 GPa is excluded, as according to the data of $M(P)$ dependence the magnetic transition to antiferromagnetic state occurs in the clusters below 1 GPa and up to 5 GPa there is a monotonous decrease of M.

[1] *E.K. Arushanov.* II_3V_2 Compounds and alloys, Prog. Crystal Growth and Charact. 1992, Vol. 25, pp. 131-201

[2] *T. Schumann, M. Goyal, H. Kim.* [et al.]. Molecular beam epitaxy of Cd_3As_2 on a III-V substrate. APL Materials. – 2016. – V. 4. – P. 126110.

[3] *S.F. Marenkin, V.M. Trukhan.* Phosphides, arsenides of zinc and cadmium. - Minsk, 2010. - C. 224

[4] *Z. Cheng, Z. Tong, L. Sihang.* [et al.]. Unexpected low thermal conductivity and large power factor in Dirac semimetal Cd_3As_2. Chin. Phys. B. – 2016. – V. 25, № 1 – P. 017202.

[5] *S. Borisenko, Q. Gibson, D. Evtushinsky, V. Zabolotnyy, B. Buchner, R.J. Cava.* Experimental Realization of a Three-Dimensional Dirac Semimetal. Phys. Rev. Lett. 113, (2014) 027603.

[6] *H. Lanpo, J. Yating, Z. Sijia* [et al.]. Pressure-induced superconductivity in the three-dimensional topological Dirac semimetal Cd_3As_2. Quantum Materials. – 2016. – V. 14. – P. 16014.

[7] *M. Neupane, S.Y. Xu, R. Sankar, N. Alidoust, G. Bian, C. Liu, I. Belopolski, T.R. Chang, H.T. Jeng, H. Lin, A. Bansil, F. Chou, M.Z. Hasan.* Observation of a three-dimensional topological Dirac semimetal phase in high-mobility Cd_3As_2. Nature Communications. 2014. – T. 5. – № 1. – C. 3786. – DOI. 10.1038/ncomms4786.

[8] *Z. Wang, H. Weng, Q. Wu, X. Dai, Z. Fang.* Three-dimensional Dirac semimetal and quantum transport in Cd_3As_2. Physical Review B. 2013. – T. 88. – №. 12. – C. 125427. – DOI. 10.1103/PhysRevB.88.125427.

[9] *A.J. Rosenberg, T.C. Harman.* Cd3As2—A Noncubic Semiconductor with Unusually High Electron Mobility // Journal of Applied Physics. 1959. – T. 30. – № 10. – C. 1621–1622. – DOI. 10.1063/1.1735019.

[10] *Z.K. Liu, J. Jiang, B. Zhou, Z.J. Wang, Y. Zhang, H.M. Weng, D. Prabhakaran, S. K. MO, H. Peng, P. Dudin, Y.L. Chen.* A stable three-dimensional topological Dirac semimetal Cd3As2, Nat. Mater. 13 (2014) 677–681, https://doi.org/10.1038/ nmat3990.

[11] *X. Wan, A.M. Turner, A. Vishwanath.* Topological semimetal and Fermi-arc surface states in the electronic structure of pyrochlore iridates, Phys. Rev. B 83 (2011) 205101, https://doi.org/10.1103/PhysRevB.83.205101.

[12] *Hong Lu, Xiao Zhang, Yi Bian, Shuang Jia.* Topological phase transition in single crystals of $(Cd_{1-x}Zn_x)_3As_2$, Sci. Rep. 7 (2017) 3148, https://doi.org/10.1038/ s41598-017-03559-2.

[13] *A.I. Ril, S.F. Marenkin.* Cadmium Arsenides: Structure, Synthesis of Bulk and Film Crystals, Magnetic and Electrical Properties (Review) / Russ. J. Inorg. Chem. 2021. V. 66. № 14. P. 2005. DOI: 10.1134/S0036023621140059.

[14] *I.F. Gribanov, A. Zavadsky, A. Sivachenko.* P. Low-temperature magnetic transformations in orthorhombic manganese arsenide. / FTN, 1979. T. 5. №. 10. C. 1219.

[15] *C. Spezzani, E. Ferrari, E. Allaria, F. Vidal, A. Ciavardini, R. Delaunay, F. Capotondi, E. Pedersoli, M. Coreno, C. Svetina, L. Raimondi.* Magnetization and microstructure dynamics in Fe/MnAs/GaAs (001): Fe magnetization reversal by a femtosecond laser pulse. / Phys. Rev. Lett. 2014. V.113. № 24. P. 247202. DOI: 10.1103/PhysRevLett.113.247202.

[16] *J. Hubmann, B. Bauer, H.S. Körner, S. Furthmeier, M. Buchner, G. Bayreuther, F. Dirnberger, D. Schuh, C.H. Back, J. Zweck, E. Reiger.* Epitaxial growth of room-temperature ferromagnetic MnAs segments on GaAs nanowires via sequential crystallization. Nano Lett. 2016. V. 16. № 2. P.900. DOI: 10.1021/acs.nanolett.5b03658.

[17] *V.M. Novotortsev, S.F. Marenkin, I.V. Fedorchenko, A.V. Kochura.* Physical and chemical bases of synthesis of new ferromagnetics from chalcopyrite $A^{II}B^{IV}C^{V}_2$. / Inorganic chemistry Journal. 2010. T. 55. № 11. C. 1868-1880. DOI: 10.1134/S0036023610110136

[18] *A.I. Ril, A.V. Kochura, S.F. Marenki*n. Proceedings of South-West State University. Series: Technics and technologies 7, 120 (2017).

[19] *L.F. Vereshchagin, E.N. Yakovlev, B.V. Vinogradov, G.N. Stepanov, K.Kh. Bibaev, T.I. Alaeva, V.P. Sakun.* High Temp.–High Press. 6, 499 (1974).

[20] *A.N. Babushkin, G.I. Pilipenko, F.F. Gavrilov.* J. Phys.: Condens. Matter. 5, 8659 (1993).

[21] *A.N. Babushkin.* High Press. Res. 6, 349 (1992).

[22] *L.G. Khvostantsev, L.P. Vereshchagin, A.P. Novikov,* High Temp.-High Pressure, 9(6), 637 (1977).

[23] *A.Yu. Mollaev, L.A. Saipulaeva, R.K. Arslanov, S.F. Marenkin.* Inorganic Materials, 37(4), 405 (2001)].

[24] *A.G. Alibekov, A.Yu. Mollaev, L.A. Saipullaeva, S.F. Marenkin, I.V. Fedorchenko, A.I. Ril.* Hall effect and magnetoresistance in the Cd_3As_2 + MnAs (30%) composite at high pressure // Journal of Inorganic Chemistry, 2017, Vol. 62, № 1, pp. 1-5.

[25] *N.V. Melnikova, A.V. Tebenkov, G.V. Sukhanova, A.N. Babushkin, L.A. Saipulaeva, V.S. Zakhvalinsky, S.F. Gabibov, A. G. Alibekov, A. Yu. Mollaev.* Thermoelectric properties of ferromagnetic semiconductor based on Dirac semimetal Cd3As2 at high pressure // Solid State Physics, 2020, Vol. 62, Iss. 6, 03,05,11.

[26] *N. Menyuk, J.A. Kafalas, K. Dwight, and J.B. Goodenough.* Phys. Rev. 177, 942 (1969).

[27] *F. Andresen, H. Fjellvåg, B. Lebech.* 43(2), 158-160 (1984).

[28] *N. Mattoso, M. Eddrief, J. Varalda, A. Ouerghi, D. Demaille, V. H. Etgens, and Y. Garreau.* Phys. Rev. B 70, 115324 (2004).